Regional Energy and Water Cycles: Transports from Ocean to Land

KEVIN E. TRENBERTH AND JOHN T. FASULLO

National Center for Atmospheric Research, Boulder, Colorado*

(Manuscript received 18 December 2012, in final form 27 March 2013)

ABSTRACT

The flows of energy and water from ocean to land are examined in the context of the land energy and water budgets, for land as a whole and for continents. Most atmospheric reanalyses have large errors of up to 15 W m^{-2} in the top-of-atmosphere (TOA) energy imbalance, and none include volcanic eruptions. The flow of energy from ocean to land is more reliable as it relies on analyzed wind, temperature, and moisture fields. It is examined for transports of the total, latent energy (LE), and dry static energy (DSE) to land as a whole and as zonal means. The net convergence of energy onto land is balanced by the loss of energy at TOA, measured by Clouds and the Earth's Radiant Energy System (CERES), and again there are notable discrepancies. Only the ECMWF Interim Re-Analysis (ERA-I) is stable and plausible. Strong compensation between variations in LE and DSE transports onto land means that their sum is more stable over time, and the net transport of energy onto land is largely that associated with the hydrological cycle (LE). A more detailed examination is given of the energy and water budgets for Eurasia, North and South America, Australia, and Africa, making use of Gravity Recovery and Climate Experiment (GRACE) data for water storage on land and data on river discharge into the ocean. With ERA-I, the new land estimates for both water and energy are closer to achieving balances than in previous studies. As well as the annual means, the mean annual cycles are examined in detail along with uncertainty sampling estimates, but the main test used here is that of closure.

1. Introduction

Global perspectives on the energy and water cycles for planet Earth are important and they set the stage for more focused aspects that are vitally important for regional climate variability and change. Biases in global values are likely to be reflected in regional values, but local biases can easily be an order of magnitude larger. Hence, examining and eliminating regional biases may help the global values. In this paper, an examination is given first of the land domain as a whole and transports of energy and water from ocean to land, and then more detailed results are given for the major landmasses, excepting for Antarctica. Included here are estimates for Eurasia, North and South America, Africa, and Australia. While we have also computed results for Greenland and Antarctica, the large nonstationary component associated with melting land ice warrants special treatment in those regions and is taken up elsewhere.

The hydrological cycle and its changes over time are of considerable interest to society, and such changes are intimately linked to the energy cycle, especially via changes in phase of water. The evaporation E, or more generally evapotranspiration (ET), of moisture in one place and the precipitation P in other places are joined via atmospheric moisture transports. On land, excess of precipitation either goes into surface water (lakes and ponds), soil moisture, and groundwater or runs off into streams and rivers and discharges into the ocean. In the ocean, excess E over P leads to more saline waters, while the reverse freshens the ocean and a balance is achieved via ocean transports. Changes in moisture storage on land can be significant in the short term (Boening et al. 2012), especially in winter in the form of snow, but changes in atmospheric storage are fairly small. Trenberth et al. (2007b) provided a synthesis of the understanding of some aspects of the global hydrological cycle and its annual cycle, both globally and for continents. Trenberth and Fasullo (2013) examine the regional energy and water cycle over North America in detail. The latter part

*The National Center for Atmospheric Research is sponsored by the National Science Foundation.

Corresponding author address: Kevin E. Trenberth, National Center for Atmospheric Research, P.O. Box 3000, Boulder, CO 80307.
E-mail: trenbert@ucar.edu

DOI: 10.1175/JCLI-D-13-00008.1

of this paper is an extension of that study to other continents.

There are many disparate datasets that pertain to aspects of the water and energy cycles and their changes over time, but it has been exceedingly difficult to synthesize them into a coherent framework that presents a physically consistent picture of these vital cycles. In this paper, we attempt to do this by examining the mean, annual cycle, and variability of the various components by taking advantage of improvements in a number of datasets. For energy, these include the top-of-atmosphere (TOA) radiation, atmospheric energy quantities, and transports from new reanalyses and the implied surface fluxes that may be evaluated using alternative surface flux products and changes in subsurface storage (section 2). For the water cycle, they include atmospheric quantities and transport from reanalyses, estimates of terrestrial runoff and water discharge into the ocean, and microgravity measurements from the Gravity Recovery and Climate Experiment (GRACE) that provide estimates of changes in water storage. The focus is on land on continental scales in order to be able to utilize integrated river discharge estimates from Dai and Trenberth (2002) and Dai et al. (2009) and avoid the complexity associated with individual river basins.

It is therefore necessary to examine how well the reanalyses replicate the energy flows. Evaluations of atmospheric energy variables and transports for land and ocean domains were given in Fasullo and Trenberth (2008a,b) and Trenberth and Fasullo (2008), and Fasullo and Trenberth (2008b) inferred ocean heat transports as a residual. Trenberth et al. (2011) evaluated eight reanalyses for water with regard to the bulk values for land and ocean as a whole and the transports from ocean to land, plus global energy, and Lorenz and Kunstmann (2012) further detailed the hydrological cycle performance in three reanalyses. Both concluded that the European Centre for Medium-Range Weather Forecasts (ECMWF) Interim Re-Analysis (ERA-I) provides the best option although some problems exist. Notably soil moisture is overestimated in ERA-I, particularly for dry land (see also Albergel et al. 2012). Scrutiny of the TOA energy imbalance here sets the stage for examining the transport of energy from ocean to land as a whole and for its components, which can be cross checked using TOA radiation observations. One of the major components is moisture (latent energy) transport and the water cycle is a key part of the energy cycle through the evaporative cooling at the surface and latent heating of the atmosphere. Hence, these aspects lead to and enable more detailed examination of continental-scale energy and water budgets and how well closure can be achieved with the latest datasets.

The conservation constraints on the energy and water budgets can be used to provide a commentary on accuracy of observational estimates. Storage of heat on land is limited by conduction, and the biggest changes are from flow and changes in water and snow cover, which are most evident seasonally. Increasing confidence in TOA and atmospheric energy budgets provides a means to estimate the surface energy budget over land as a residual.

The most comprehensive terrestrial freshwater discharge data come from the synthesis of 925 of the largest rivers with modeling of the missing data in space and time to produce time series for 1948–2004 (Dai et al. 2009). Unfortunately it has not been possible to update these series and river gauge data are degrading. Accordingly, attention is given to the decadal variability estimates from this dataset. Syed et al. (2009) made GRACE-based estimates of terrestrial freshwater discharge for the limited period of 2003–05 while using the National Centers for Environmental Prediction–National Center for Atmospheric Research (NCEP–NCAR) reanalysis for atmospheric transports. The latter suffer from multiple problems (Trenberth et al. 2005, 2011) and the more recent reanalyses provide superior estimates of the atmospheric component. Alternative estimates of water discharge from land have been given by Syed et al. (2010) for 1994–2006 based upon changes in the ocean as seen in the ocean mass and sea level changes plus precipitation and surface evaporation flux estimates over ocean, but these have quite large uncertainties (e.g., Trenberth et al. 2007a, 2011) and they are not constrained by conservation principles. van der Ent et al. (2010) provide new estimates of the movement of atmospheric moisture and how much is recycled in various regions but depend a lot on model estimates of recycling. The lifetime of moisture in most models is too short (Trenberth et al. 2011).

Over land, Jiménez et al. (2011) and Mueller et al. (2011) evaluated a set of global datasets of ET from remote sensing, land surface models (LSMs), reanalysis, and climate models and found the uncertainties to be close to 50% of total mean annual values. Vinukollu et al. (2011) further evaluated available ET estimates from many sources and found issues with continuity in time and likely biases. Large differences were found between satellite-based estimates versus surface meteorological-based estimates and output from several models driven by the meteorological input. The spread from the different models contributed to the uncertainty.

A comprehensive approach to estimating the terrestrial water cycle (Sahoo et al. 2011) albeit with satellite data used multiple satellite remote sensing and ground-based products for 2003–06 that were reconciled and merged into a single best estimate for 10 river basins based on uncertainty estimates. With the original data,

closure of the water budget was not achievable and errors were on the order of 5%–25% of the mean annual precipitation. However, the merging into a physically constrained budget resulted in the biggest errors being assigned to satellite precipitation products. Using individual river basins enables observations of river discharge to be utilized but the complex topography that bounds a basin may contribute to errors via the GRACE data owing to its footprint size and ''leakage'' across the domain borders. Pan et al. (2012) proposed a systematic method of synthesizing all water-related data and model simulations and applied the method to 32 globally distributed major river basins for 1984–2006. These promising results nonetheless depend on the assignment of errors to each dataset.

Here we overcome the problem of domain borders of each river basin to a large degree but at the expense of uncertainty in the integrated river discharge into the ocean not being concurrent in time.

2. Methods and data

The atmospheric conservation of moisture equation when vertically integrated in flux form is

$$\frac{\partial w}{\partial t} + \nabla \cdot \frac{1}{g} \int_0^{p_s} \mathbf{v} q \, dp = E - P, \tag{1}$$

where q is the specific humidity, $w = (1/g) \int_0^{p_s} q \, dp$ is the precipitable water (total column water vapor), E is the surface evaporation, and P is the net surface precipitation rate. In addition to water vapor, atmospheric liquid water and ice components are also included, although these are mostly small. The whole equation can be expressed also in terms of energy by multiplying by L, the latent heat of vaporization. Because the tendency term is small, the primary balance is thus between the freshwater flux $E - P$ and the moisture divergence.

The surface water conservation equation is

$$\partial S/\partial t = P - E - R, \tag{2}$$

where S is the subsurface storage of water substance and R is the runoff. Hence, if the changes in atmospheric and surface storage are negligible, the balance is between atmospheric moisture convergence and runoff.

The vertically integrated energy budget is made up of net TOA radiation R_T, the convergence of energy by the atmospheric winds, and the net surface flux of energy F_s. The net radiation in turn consists of the incoming absorbed shortwave radiation (ASR) and the outgoing longwave radiation (OLR), R_T = ASR − OLR. The total atmospheric energy (TE) transport is made up of dry static energy (DSE), latent energy (LE), and kinetic energy (KE) components, but the latter contribution is small (Trenberth and Stepaniak 2003a). Together the moist static energy (MSE) is MSE = DSE + LE. The changes in storage of atmospheric energy, $\partial \mathrm{TE}/\partial t$, must also be accounted for. Although estimates of the surface flux of energy exist, with components from net radiation and sensible and latent heat fluxes, here we estimate this as a residual of the other components, symbolically given as

$$F_s = R_T - \nabla \cdot \mathbf{v}\mathrm{TE} - \partial \mathrm{TE}/\partial t, \tag{3}$$

where $\nabla \cdot \mathbf{v}\mathrm{TE}$ represents the divergence of the vertically integrated horizontal transport of total energy by the velocity $\mathbf{v}$ (for details, see Trenberth and Stepaniak 2003a). Note that here F_s is directed downward (opposite in convention to Fasullo and Trenberth 2008a,b).

For energy, we make use of Clouds and the Earth's Radiant Energy System (CERES) TOA observations, Energy Balanced and Filled (EBAF) v6.2r (Loeb et al. 2009), as part of the energy cycle and hence this limits the timeframe from March 2000 to the present. For vertically integrated groundwater and soil moisture, we use GRACE data (e.g., Syed et al. 2009, 2010) which are available only after March 2002 for 66°N–66°S, and we use the recently reprocessed GRACE data from Landerer and Swenson (2012) for 2003–10 based on the so-called RL04 release. For river discharge, the synthesized river discharge data (Dai et al. 2009) are used but these are only available as time series up to 2004, limiting our ability to close the water cycle as long time series. However, we will use these values as constraints on the mean annual cycle in terms of subsurface water storage changes, and the interannual and decadal variability is assessed to place uncertainties on the values.

Recent atmospheric reanalyses have improved markedly over earlier ones but all still have residual problems that must be accounted for. The reanalyses have the major advantage of postprocessing all of the data that are available after considerable quality control in a consistent data assimilation system. However, in the absence of a perfect model and observations, as the model predicted state at any time is adjusted by the available observations to produce an analysis increment, quantities such as water and energy are not conserved (but are in nature). Moreover, the sea surface temperatures (SSTs) are specified as boundary conditions for the reanalyses, thereby providing an infinite reservoir of heat and water for the overlying atmosphere. Further, the changing observing system introduces noticeable inhomogeneities into the apparent climate record in reanalyses (Robertson et al. 2011; Trenberth et al. 2011), and energy and water are not conserved in the atmospheric reanalyses, although some are better at this than others.

Model generated estimates of surface water fluxes of precipitation and evaporation were used by Trenberth et al. (2011) to compute the net sources of atmospheric moisture $E - P$ over the ocean and the net sink $P - E$ over land, and these were compared with the analyzed transports of moisture from ocean to land and the estimated runoff from land to ocean. Large discrepancies indicate the shortcomings of some models and the assimilation systems. In particular, the more recent reanalyses from ERA-I (Dee et al. 2011) and Modern-Era Retrospective Analysis for Research and Applications (MERRA) (Rienecker et al. 2011) use four-dimensional variational analysis (ERA-I) or an incremental update procedure (MERRA), which largely removes spinup of the hydrological cycle that is present in other reanalyses. However, large spurious changes associated with the changing observing system greatly influence the precipitation and some related variables. Bosilovich et al. (2011) have carried out a comprehensive evaluation of some reanalyses with a focus on MERRA and the global energy and water cycles. The transports of moisture from ocean to land were found to be much more resilient to such changes and more reliable and consistent across reanalyses than P and E estimates (Trenberth et al. 2011). Accordingly, in this paper we go a stage further and examine the moisture transports and their convergence over land to examine regional aspects while assessing their merit using physical constraints associated with other datasets.

3. Transports of energy and water from ocean to land

a. Global land

In examining transports from ocean to land, the resolution of the data can make a difference because it affects the delimiters of the land–ocean coastline. How one defines land can also make some differences and here we include permanent ice shelves as land. By moving from T42 resolution for the Earth Radiation Budget Experiment (ERBE), as in Fasullo and Trenberth (2008a), to T63 resolution here, there is an increase in transport from ocean to land of 0.4 PW. This comes from much improved definition of many islands, such as Japan and New Zealand. In our calculations, we ensured that the area of land is the same across all reanalyses and we used the same land–sea mask.

To frame the analysis, it is worthwhile outlining the a priori expectations for transports of energy from ocean to land. In the extratropics, the Northern Hemisphere dominates and strong westerlies in winter transport heat and moisture from ocean to land, highlighting the maritime versus continental influences. In summer, land is typically warmer than the ocean and sea breezes may develop that transport heat from land to ocean although compensated by moisture transport to land as part of the hydrological cycle. Indeed, in lower latitudes in monsoons, there is a transport of moisture from ocean to land as LE that gives rise to diabatic heating in the monsoon rains, and the monsoon circulation itself transports DSE from land to ocean in summer. A characteristic of these kinds of flows is a very large cancellation between LE and DSE transports (Trenberth and Stepaniak 2003b) with a small net transport from land to ocean. Overall there must be a moisture transport from ocean to land as part of the hydrological cycle. In addition, globally there is compensation between the two hemispheres.

Fasullo and Trenberth (2008a) provided estimates of the annual mean net energy flow from ocean to land as 2.2 ± 0.1 PW (±2 sigma) from the NCEP–NCAR reanalysis and the 40-yr ECMWF Re-Analysis (ERA-40). Values rose to 5 PW in the Northern Hemisphere winter and reversed somewhat in the northern summer. Interannual variability of monthly means was order ±1 PW, with only small (order of 0.2 PW) differences between the two reanalyses.

Based on streamflow discharge into the ocean (Dai and Trenberth 2002; Dai et al. 2009), the moisture transport from ocean to land is $40 \times 10^3\,\mathrm{km^3\,yr^{-1}}$ [or 40 Eg $\mathrm{yr^{-1}}$, which is 1.3 Sv ($1\,\mathrm{Sv} \equiv 10^6\,\mathrm{m^3\,s^{-1}}$)]. These values include crude estimates for Antarctica ($2.6 \times 10^3\,\mathrm{km^3\,yr^{-1}}$), and so the rest of land value is $\sim 37.3 \times 10^3\,\mathrm{km^3\,yr^{-1}}$ overall. For the 1990s, when the impact of Mount Pinatubo dropped values down somewhat owing to reduced solar flux (Trenberth and Dai 2007), the estimate is $\sim 39 \times 10^3\,\mathrm{km^3\,yr^{-1}}$. The uncertainties in these estimates are not well determined. The temporal variability from 1948 to 2004 has a standard deviation of $0.98 \times 10^3\,\mathrm{km^3\,yr^{-1}}$, giving an uncertainty in a decade mean of about $\pm 0.6 \times 10^3\,\mathrm{km^3\,yr^{-1}}$ (2 standard errors). However, the structural uncertainty is likely larger and best determined by examining the closure.

First, to provide some overall context for interpreting energy flow results from reanalyses, Fig. 1 shows the net TOA radiation into Earth from several reanalyses. Shown are results from the NCEP–NCAR reanalysis [labeled as NCEP–NCAR Global Reanalysis 1 (NCEP-1)], the Japanese Reanalysis Project (JRA), ERA-40, NCEP Climate Forecast System Reanalysis (CFSR), MERRA, and ERA-I (see Trenberth et al. 2011). Although the exact observed values are not known, the net imbalance after 1994 is about 0.7–0.9 $\mathrm{W\,m^{-2}}$ (Trenberth 2009; Trenberth et al. 2009; Loeb et al. 2009; Hansen et al. 2011), with a slight drop in the 2000s by 0.10–0.15 $\mathrm{W\,m^{-2}}$ owing to the quiet sun. The Mount Pinatubo eruption caused a major drop in incoming

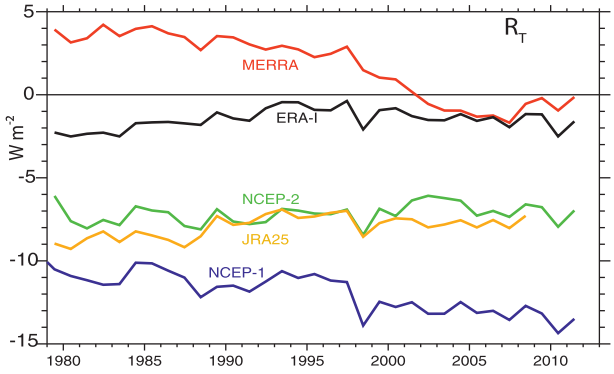

FIG. 1. Net annual mean radiative imbalance downward R_T ($W\,m^{-2}$) at TOA from several atmospheric reanalyses.

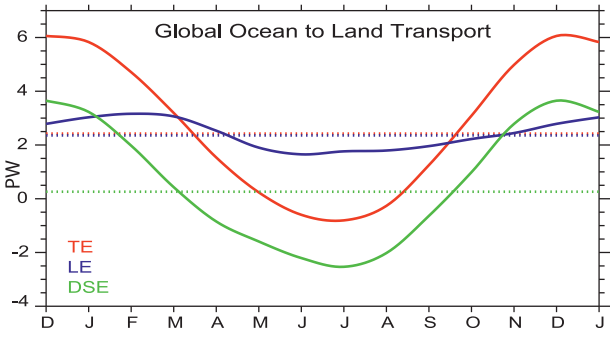

FIG. 2. Global transport of energy from ocean to land from ERA-I for 1979–2010. Mean annual cycle is for the TE, LE, and DSE, with the annual mean for each dotted.

radiation in 1991 (e.g., Trenberth and Dai 2007), but this is not present in any of the atmospheric reanalyses, although it features prominently in an ocean reanalysis (Balmaseda et al. 2013). Clearly the imbalance is positive, as warming is readily apparent (Solomon et al. 2007), but both the absolute values and the changes over time in atmospheric reanalyses have little or no relationship to the actual values expected, and values can be off by $10\,W\,m^{-2}$. ERA-I values are the most stable and plausible and closest to correct but with an offset of about $-3\,W\,m^{-2}$.

The energy transports from ocean to land from ERA-I for 1979–2010 are examined (Fig. 2) for the mean annual cycle. Given are the contributions from LE, DSE, and the total, which also includes a very small component from kinetic energy. The annual mean DSE transport is close to zero, but it exhibits a large annual cycle ranging from +3 PW in January to −3 PW in July. There is a small annual cycle to LE with a peak in February and an annual mean of about 2.5 PW. Accordingly, the TE transport also averages 2.5 PW but has a large annual cycle. This is slightly larger than found by Fasullo and Trenberth (2008a), and the differences result mainly from higher resolution and improved land–sea definition.

The 12-month running mean transport of energy from ocean to land shows quite a large spread among reanalyses (Fig. 3), which is not altogether surprising given the large and varying impacts of changes in the observing system on most of the reanalyses (Trenberth et al. 2011). Shown are results from NCEP-1, JRA, ERA-40, CFSR, MERRA, and ERA-I. Problems in the archive prevented calculations of MERRA DSE transports.[1] The least agreement is for DSE and problems are known to occur in NCEP-1, JRA, and CFSR, which were all greatly affected, especially by the 1998–2001 transition from Television and Infrared Observation Satellite (TIROS) Operational Vertical Sounder (TOVS) to Advanced TOVS (ATOVS), and ERA-40, which was beset with problems associated with and following the Pinatubo eruption. Surprisingly, there is more agreement with the LE transports in terms of both sharp drops in 1991 following the Mt Pinatubo eruption and in 1997/98 with the major El Niño event while exhibiting a general slight upward trend.

The transport of total energy, including kinetic energy, from ocean to land (Fig. 4) is similar to that for MSE. However, now we add the observed loss of net energy to space from ERBE and CERES observations, where the uncertainty in absolute value associated with the overall energy imbalance is less than 0.2 PW. The mean value is about 2.8 PW, and it is fairly stable over time, with only the ERA-I values being somewhat close and of similar character in terms of variability. Figure 1 suggests that the ERA-I values could be off by $3\,W\,m^{-2}$, which is 1.5 PW globally. However, the transport data relies on quite different variables to the radiative TOA computation. Hence, an offset by 0.3 PW in the ocean to land transport is much less than the TOA imbalance but not surprising. The CERES values may also be questionable, as the interannual variability of the global values does not agree very well with the variability from year to year in ocean heat content (Loeb et al. 2012). For the latter, the error bars are so large as to make apparent agreement meaningless. The apparent discrepancies between TOA net radiation and ocean heat content variations result in ''missing energy'' (Trenberth and Fasullo 2010), but this may be resolved when the deeper ocean heat variations are included (Balmaseda et al. 2013).

Figure 5 presents the variability in the anomalies of the main contributing terms for ERA-I. Quite striking

[1] In the corrector segment in MERRA, heat fluxes are adjusted to compensate for the analysis increment, and the archived result is not the analyzed value, so that the apparent value has the wrong sign (M. Bosilovich 2012, personal communication).

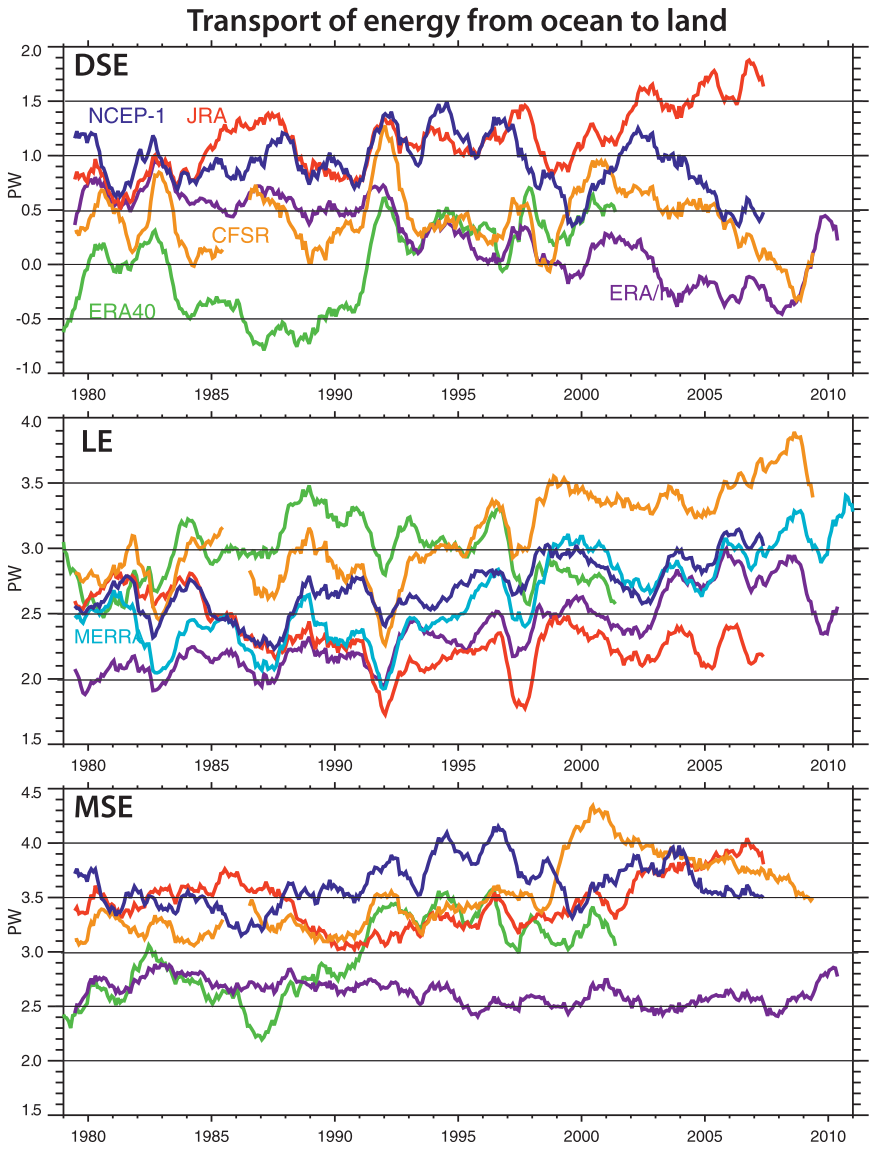

FIG. 3. Transport of (top) DSE, (middle) LE, and (bottom) MSE from ocean to land from various reanalyses as labeled as 12-month running means in petawatts.

variations are present from 0.7 to −0.7 PW in both LE and DSE but with large cancellation, and much smaller variations occur in TE transport. The cancellation suggests a dominance of lower latitudes as will be shown later (see Fig. 6).

In general it is expected that there is an increase in precipitation over the tropical Pacific Ocean during El Niño events and more drought on land and the reverse during La Niña (Gu et al. 2007), which would signify an increase in LE transport onto land during La Niña. This happened in a major way in 2010/11 by enough to lower sea level by some 5 mm (Boening et al. 2012) (not quite shown in Fig. 5). The downward peaks in LE transport (Fig. 5) consistently occur in El Niño years. In addition there is a volcanic signal (Gu et al. 2007; Trenberth and Dai 2007) resulting in less land precipitation, especially following the Mount Pinatubo eruption in 1991.

Overall, then, it appears that there is a net transport of energy from ocean to land that is almost entirely made up of the moisture transport for the annual mean. However, there are large seasonal variations superposed. Moreover, there are large ENSO and lower-frequency variations.

Before advancing to examine the regional aspects, the global mean land values of several variables are presented in Table 1. This gives the monthly mean and annual mean

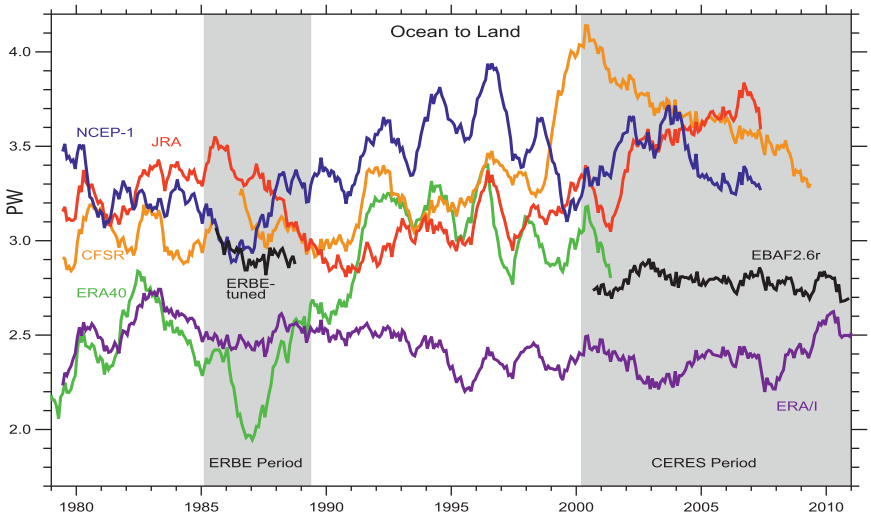

FIG. 4. Transport of total energy from ocean to land from various reanalyses as labeled as 12-month running means in petawatts. Also shown are the ERBE and CERES radiation from land to space and the gray shading shows the time for observations from each.

values for precipitation from the Global Precipitation Climatology Project (GPCP), precipitation and evapotranspiration from ERA-I, runoff from Dai and Trenberth (2002), and moisture convergence and $E - P$ (moisture budget) from ERA-I. These values are surprisingly similar to those presented by Trenberth et al. (2007b), which were based on results from a land model forced with observed precipitation and estimates of other atmospheric forcings. Both precipitation and ET peak in July because of the dominance of Northern Hemisphere land. Atmospheric moisture convergence, however, peaks in February, in the southern summer associated with the Southern Hemisphere land, while the annual cycle is small in the Northern Hemisphere. Regional details are given below.

b. *Meridional annual cycle*

As an update and extension to Fasullo and Trenberth (2008b), Fig. 6 presents the latitude–time section for land for the total mean annual cycle for R_T, the divergence of LE and DSE, and the net surface flux F_s. The large compensation between the DSE and LE contributions throughout the tropics is readily apparent (Trenberth and Stepaniak 2003b), and the large annual cycle in DSE convergence in winter and divergence in summer is evident over both hemispheres (to 50°S in the Southern Hemisphere). The net surface flux is the residual and is mostly small but gets up to 45 W m^{-2} in the northern high latitudes (Fig. 6).

For water-related quantities, Fig. 7 presents the annual cycle over land for P and runoff from ERA-I, $P - E$ from the atmospheric moisture budget, and the GRACE changes in storage. These latter three should sum to zero if the water budget is closed. It is not. Here the runoff from ERA-I is not the observed values used elsewhere in this paper, and the timing, in particular, differs from the observations. The implied change in storage from ERA-I is shifted by at least 1 month earlier relative to the GRACE-implied values. The $P - E$ panel is similar to the divergence of LE panel in Fig. 6 as the difference is an atmospheric storage tendency term. The excess of E over P in the subtropics in winter months can only occur if there a release of moisture from the soils and groundwater, as is found in the $\partial S/\partial t$ panel. The drying of northern continents is also evident in summer.

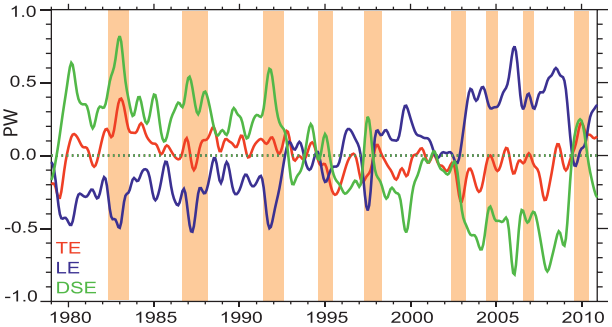

FIG. 5. Global transport of energy from ocean to land from ERA-I for 1979–2010 in petawatts and monthly anomalies smoothed with a 13-point filter that reduces less than annual fluctuations (Trenberth et al. 2007a) for the TE, LE, and DSE. Also shown (shaded peach) are the El Niño events as denoted by the ocean Niño index from the National Oceanic and Atmospheric Administration.

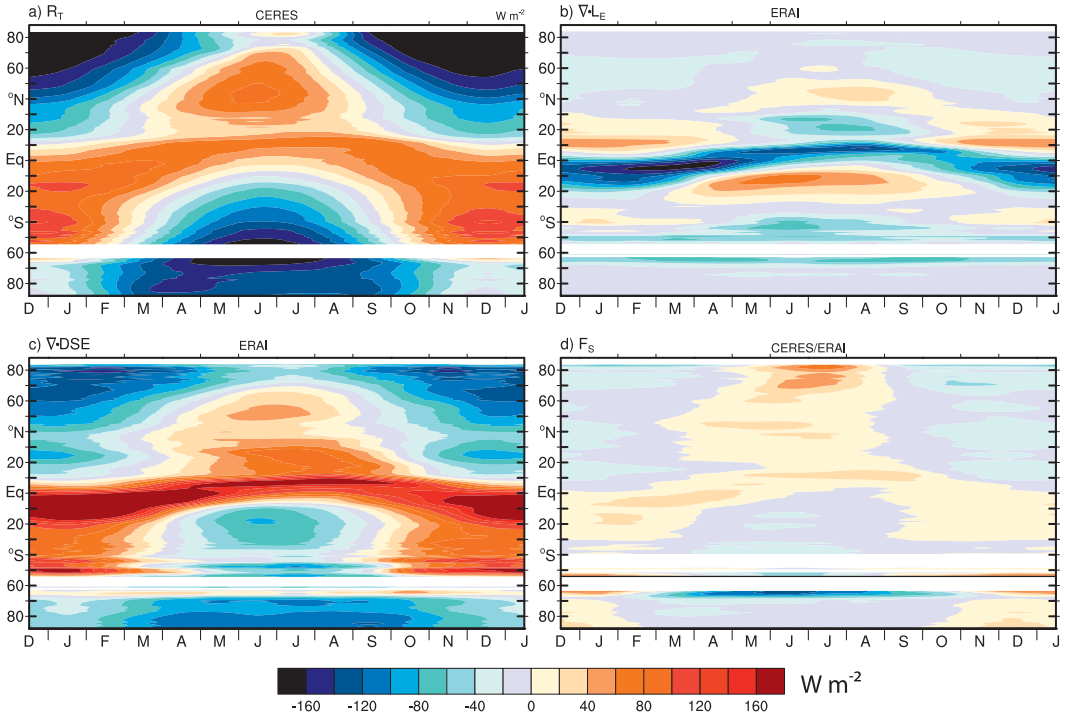

FIG. 6. Mean annual cycle of the zonal mean energetic terms for land (W m^{-2}) averaged for 2000–10. Given are net TOA radiation downward R_T, the divergence of LE and DSE, and the implied surface flux F_s downward.

c. *Continental regions*

The energy and water budgets for North America have been outlined in detail in Trenberth and Fasullo (2013), who also explored the interannual variability of the moisture budget for that region in terms of the overall moisture convergence and how well it was replicated in reanalyses. Here we document the various components of both for the annual mean and annual cycle for Eurasia, North and South America, Australia, and Africa. North America is included for completeness.

Hence there are five sets of figures, one for each region (Figs. 8–12). Each figure consists of two major parts devoted to the energy cycle (left) and the water cycle (right); within those, at the right there are the annual mean values as vertical bars and the departures from the annual mean at the left. Note that the vertical scales differ among the regions. For energy, included are R_T, ASR, and OLR from CERES; the divergence of TE, DSE, and LE from ERA-I; the tendency term; and then the residual as F_s. For water, P and E from the model reanalysis are included along with $P - E$ from the moisture budget. The P from GPCP (Huffman et al. 2009) is also included as well as the moisture convergence term. In addition, the tendency in total groundwater storage from GRACE is given along with river discharge estimates for the continent and their sum as a residual.

In the figures, the spread around the mean annual cycle is determined from the interannual variability and given as one standard deviation (not a standard error). Hence, the standard error of the mean values depends upon the number of years. Because the river discharge is for a different period, we made use of the full 1948–2004

TABLE 1. Monthly and annual mean land values for 2000–10 precipitation P from GPCP; precipitation P, evaporation E, moisture convergence QConv, and $P - E$ (from moisture budget) from ERA-I; and runoff R (mm day^{-1}) for 1990–2005 from Dai et al. (2009). The maximum value is in boldface and the minimum is in italics. A value of 1 mm day^{-1} is equivalent to 4.3 PW of latent energy or 5.4×10^4 km^3 yr^{-1}.

Month	P GPCP	P	E	R	QConv	$P - E$
Jan	2.14	2.12	*1.25*	*0.49*	0.80	0.79
Feb	2.18	2.15	1.29	0.52	**0.84**	**0.81**
Mar	2.15	2.15	1.39	0.53	0.78	0.75
Apr	1.99	2.11	1.54	0.57	0.64	0.59
May	*1.96*	2.11	1.69	0.73	0.52	0.45
Jun	2.13	2.28	1.85	**1.02**	*0.47*	*0.39*
Jul	**2.31**	**2.44**	**1.91**	0.89	0.49	0.44
Aug	2.23	2.36	1.78	0.81	0.48	0.51
Sep	2.07	2.25	1.60	0.76	0.51	0.59
Oct	1.97	2.13	1.43	0.65	0.58	0.64
Nov	1.98	*2.07*	1.33	0.53	0.61	0.66
Dec	2.09	2.11	1.26	0.50	0.75	0.76
Annual	2.10	2.19	1.53	0.67	0.62	0.61

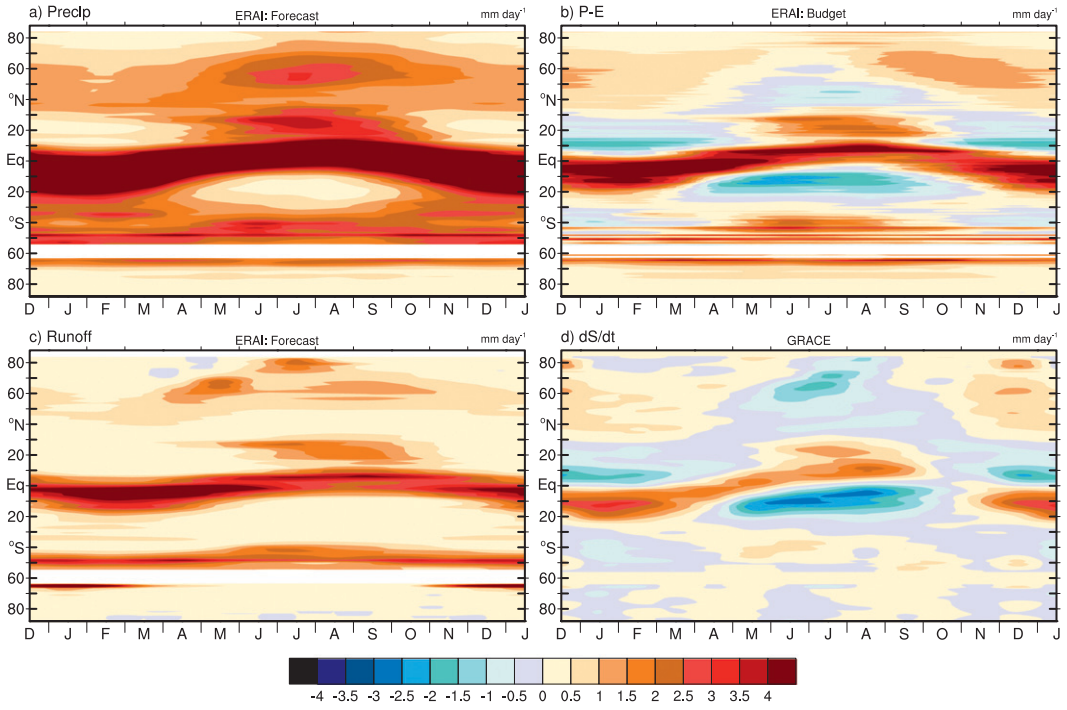

FIG. 7. Zonal mean moisture budget terms for land. Given are the (a) precipitation from ERA-I, (b) $P - E$ from the atmospheric moisture budget, (c) land river discharge and runoff into the oceans from ERA-I for 2000–10, and (d) GRACE mean monthly rates of change in water storage (mm day^{-1}) for 2003–10.

record to compute the standard deviation of 8-yr means in estimating a standard error of the residual of the water budget. Note that, to compare the values in Figs. 8–12, which are per unit area, with Fig. 2, it is necessary to also account for the land area.

For Eurasia and North America (Figs. 8, 9), there is some similarity. OLR exceeds ASR and there is a net sink of energy made up largely by a combination of convergence of DSE and LE. OLR peaks late in summer following temperature, while ASR peaks in June with the solstice, so that the annual cycle of R_T peaks earlier and with lower values than ASR. In the annual cycle, latent energy divergence plays very little role for Eurasia because of large compensating effects in the Asian monsoon and extratropical moisture transports. In both landmasses, the annual F_s value is less than 4 W m^{-2} and, as an indication of the error in closure, it is quite small. However, there is a distinct annual cycle in F_s associated with the heating up and drying of the land after the spring equinox peaking about June. Maximum cooling occurs in November.

Owing to the large monsoon contribution to Eurasia, the water cycle differs somewhat between the two landmasses (Figs. 8, 9). Precipitation peaks sharply in July in Eurasia, but the peak is drawn out more in North America. ET has a sharp maximum in both regions in late June, reflecting the energy and water availability. In Eurasia, P exceeds E from June through September while river discharge peaks in June as the land also dries out in terms of water storage. The latter is more distinctive and larger in amplitude in North America, where $P > E$ replenishes groundwater from October through February. The annual mean water imbalance, which should be close to zero, is indeed extremely small in both regions and even its annual cycle is quite small, although the nature of the annual cycle variations is suggestive of slight errors in GRACE.

In the Southern Hemisphere, Australia and South America (Figs. 10, 11) have somewhat opposite annual cycles to the northern continents and both have strong monsoon components. In South America, the annual cycle of moisture convergence is huge compared with other regions and the large net convergence of atmospheric moisture feeds the mighty Amazon River flows, which is seen as the 1.8 mm day^{-1} runoff value (Fig. 11). The monsoon component makes for relatively much larger interannual variability than in the extratropics, especially associated with ENSO (Fig. 5). For energy, both continents have a tiny excess of energy and net transport of energy to the oceans. The closure is excellent for Australia but exceeds 4 W m^{-2} for South America, highlighting uncertainties in some data.

Australian rain (Fig. 10) mostly evaporates or goes into seasonal storage, with the runoff small for the annual

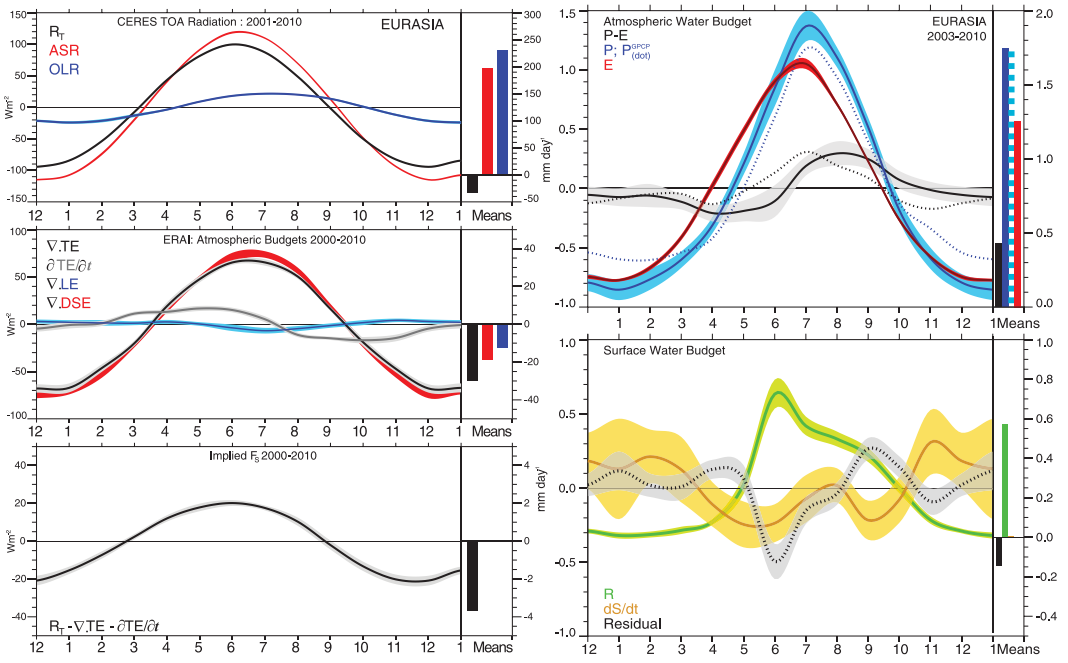

FIG. 8. (left) Regional energy budget terms (W m^{-2}) and (right) water budget terms (mm day^{-1}) for Eurasia with the annual means as bars on right side of the departures from the annual means. The shading denotes one standard deviation spread about the mean. (top left) TOA radiation for ASR (red), OLR (blue), and net (R_T) (black) for 2000–10; (middle left) divergence of total energy (black), latent energy (blue), and dry static energy (red) and the rate of change in total energy (gray) for 2000–10; and (bottom left) the residual, which is the implied surface energy flux into the earth from the net downward radiation minus the divergence of total energy minus the change in energy storage. (top right) Precipitation from ERA-I (blue) and GPCP (blue dotted or blue dashed at right), evaporation from ERA-I (red), $P - E$ from the moisture budget (black), and the convergence of the latent energy flux (black dotted), all for 2003–10. (bottom right) River discharge R into the oceans (green) for 1990–2004, change in water storage S on land (orange) for 2003–10, and the residual (black dotted or solid at right) computed as $P - E - dS/dt - R$. For the latter, the shading depicts ±1 standard error of the mean.

mean and each month as well. In contrast, the annual runoff is huge in South America (Fig. 11) and there is a distinct annual cycle. The annual cycle of groundwater storage is also very substantial. Both ERA-I and MERRA monsoon precipitation were shown to be too low in the southern Amazon in January (Trenberth et al. 2011). In Australia, there is a residual to the water balance associated with too much evaporation in ERA-I (Trenberth et al. 2011; Albergel et al. 2012). In South America, there is a spurious annual mean surplus of water most likely associated with an underestimate of streamflow (Dai et al. 2009).

In Africa (Fig. 12), there is a strong semiannual cycle to the net radiation and energy transports associated with the fact that Africa straddles the equator and has a double monsoon. The land area is skewed to the north, however. Again, there is large interannual variability associated with the monsoon rains and ENSO. Peak absorbed and net radiation is in the northern spring and autumn, as the monsoon cloudiness reduces amounts at the solstices. There is a net annual surplus of radiation of order 20 W m^{-2} that is transported offshore by the monsoon circulation even as moisture is transported onto land. There is no annual cycle in the surface heat storage F_s, but annual mean closure of the energy budget exceeds 4 W m^{-2} as a spurious residual.

For water in Africa (Fig. 12), the broad peak from August to March in rainfall is countered by a sharp reduction in June, prior to the northern monsoon. Moisture convergence peaks in August and is a minimum in May, and discrepancies between rainfall estimates highlight data uncertainties. Storage of water peaks in July–August, and there is a small annual cycle in river discharge, peaking late in the year. The residual is quite large seasonally, suggesting uncertainties in several quantities, especially from August to November.

4. Conclusions

In this paper, we first show the merits and shortcomings of the reanalyses with regard to TOA radiation and transports of energy and water from ocean to land, and

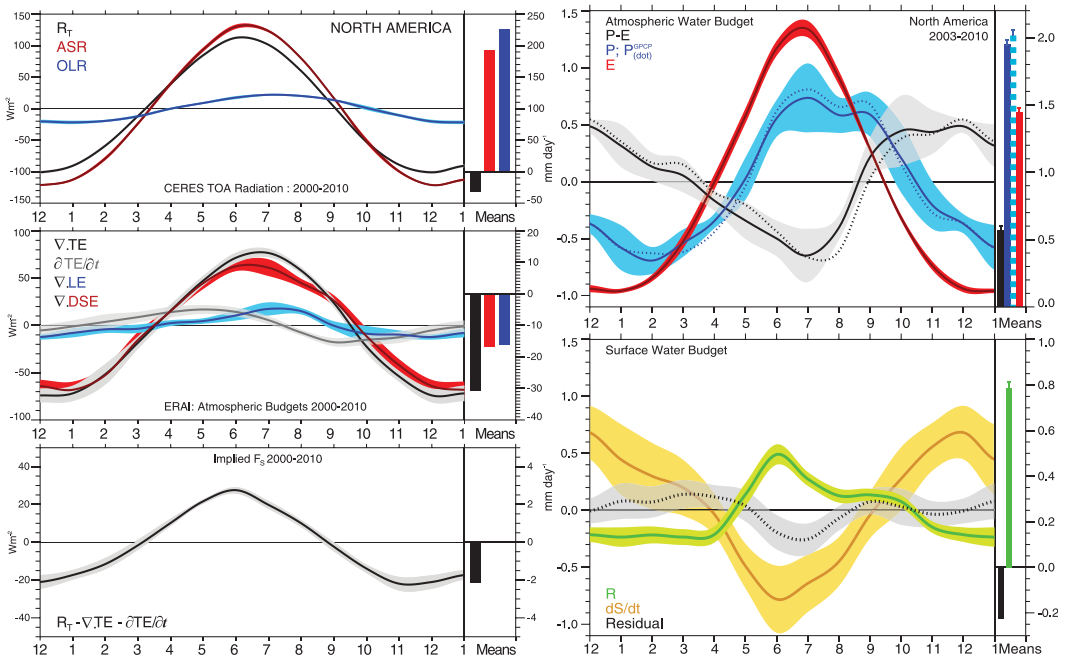

FIG. 9. As in Fig. 8, but for North America.

then we exploit them as best we can to provide insights into regional energy and water cycles. There is a net transport of energy from ocean to land that is almost entirely made up of the moisture transport for the annual mean. However, there are large seasonal variations superposed associated with DSE transports: large energy transports (6 PW) onto land in northern winter but small net transports from land to ocean in northern summer. Moreover, there are large ENSO variations, with smaller transports of moisture onto land during El Niño events. Large differences exist among results from different reanalyses and even the most stable and best (ERA-I)

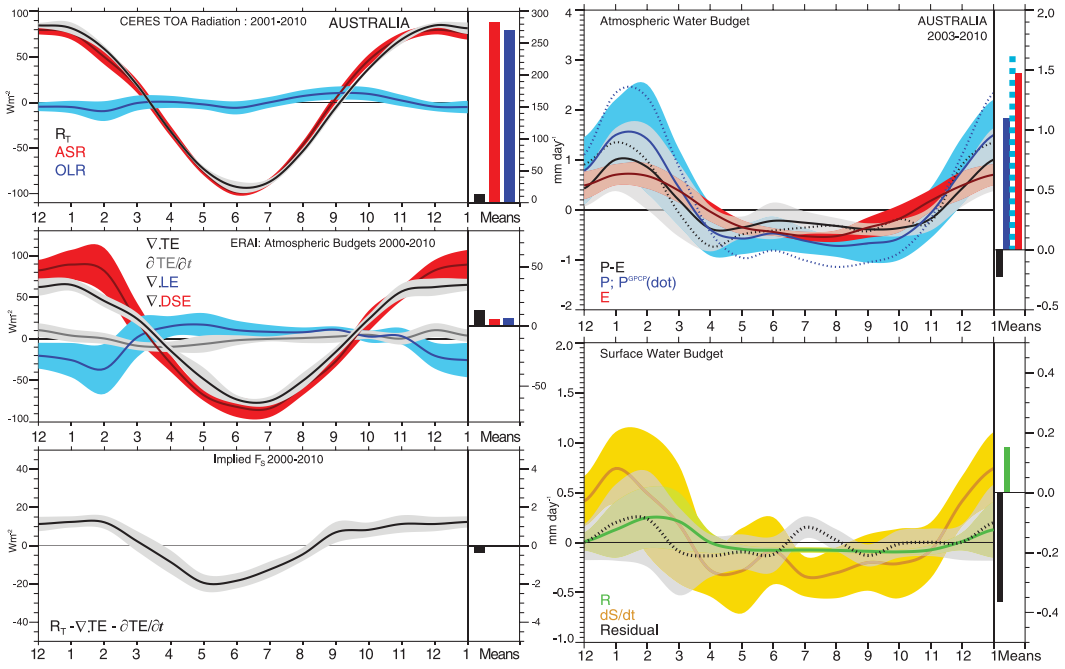

FIG. 10. As in Fig. 8, but for Australia.

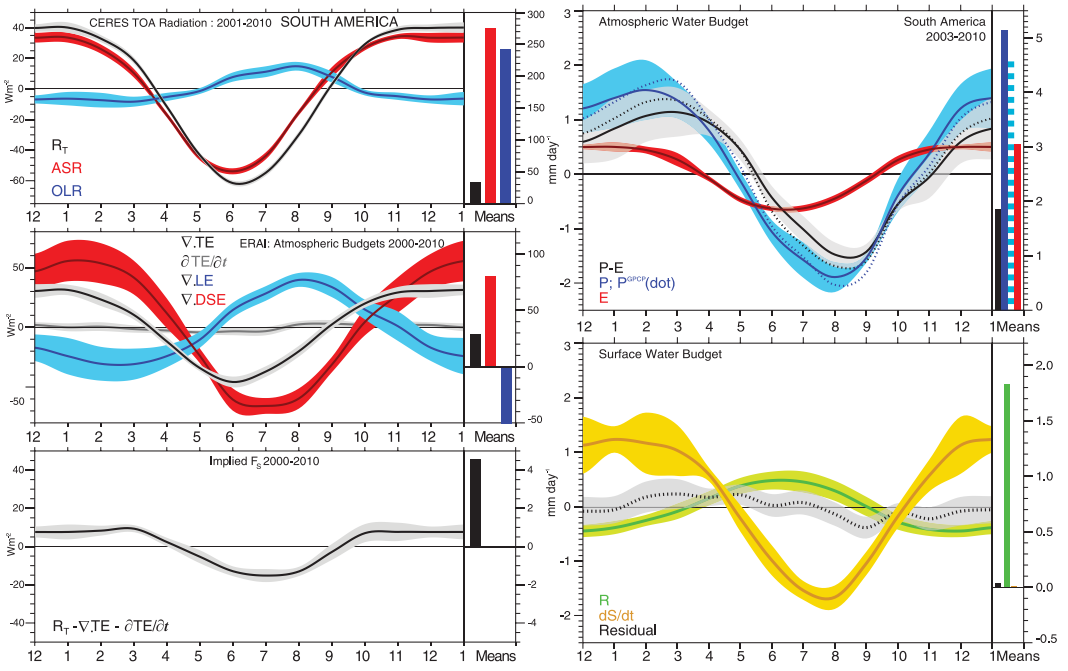

FIG. 11. As for Fig. 8, but for South America.

contains spurious trends in LE transport onto land, as discussed below. Nonetheless, for land as a whole and for the large continental regions described here, the description of the annual means and the mean annual cycle is now quite good and these signals are much larger than the estimated uncertainties.

There is a wealth of information contained in the figures that are only partly described here. Using ERA-I, a reasonably physically consistent picture emerges as to the mean and annual cycles of energy and water flows from ocean to land in the atmosphere and the continental-scale energy and water budgets on land. In other

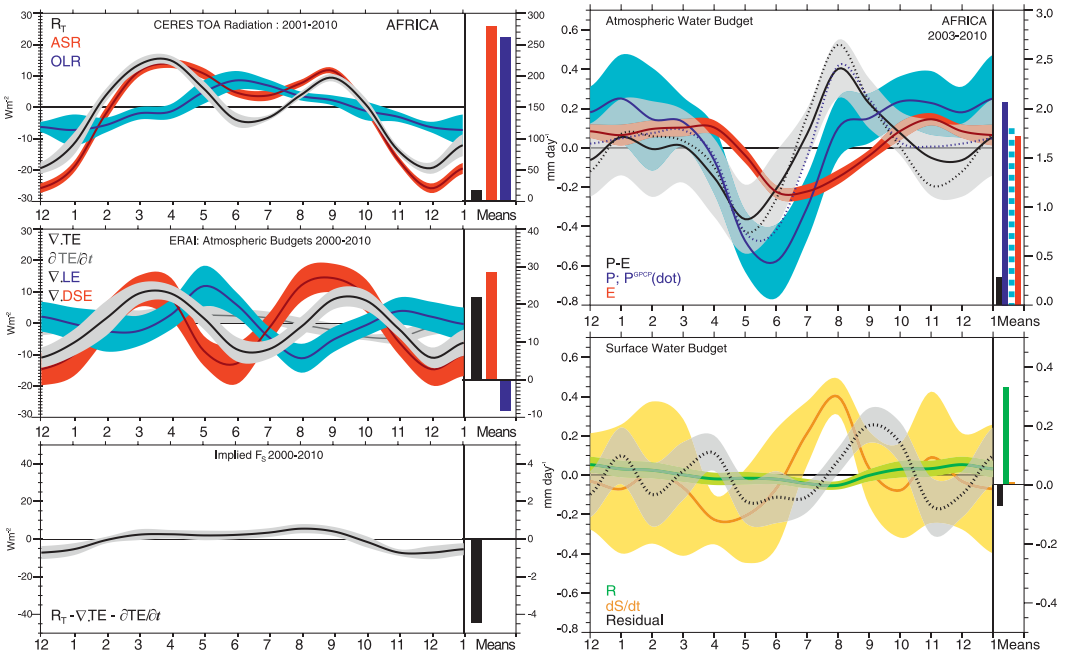

FIG. 12. As in Fig. 8, but for Africa.

words, the closure of the regional energy budgets is quite good and it is mainly in regions of known lower quality observations (Africa and South America) where problems are apparent, although arid regions such as Australia can be improved as well. This does not mean the closure exists locally on land as there are compensating errors.

The Global Precipitation Climatology Centre (GPCC; Schneider et al. 2013) has released a new land precipitation version and shows substantial differences with ERA-I precipitation and some modest differences with GPCP. The latter are mainly over Africa and South America, as well as throughout Indonesia, highlighting data issues. However, differences are bigger with ERA-I but often of mixed sign, so that they cancel to some degree on a continental basis.

More generally, we have evaluated aspects of energy and moisture flows from ocean to land and TOA energy imbalances in a number of atmospheric reanalyses and found that most contain unacceptable errors. None of the reanalyses treat volcanic eruptions and aerosol in the atmosphere at all, and the energy imbalance has the wrong sign and mostly unreliable variability. In reanalyses, this is not a tuned quantity as it is in climate models and, even if it were, it would be upset by the assimilation of data (analysis increments) and fixed SSTs that provide an infinite source or sink of energy, while the oceans always provide sources of moisture.

As noted previously, the total flow of energy is much more stable than its constituent parts. By far the largest components are DSE and LE, which are strongly negatively correlated in the tropics, in particular. This is especially characteristic of monsoons, where low level winds transport moisture onto warm land, which realizes latent heat when condensation occurs, but there has to be a net transport of energy from land to ocean to drive the monsoon circulation. While the land–sea contrast in temperature sets the stage, much of the heat comes from the latent energy. By far the largest interannual variability is also in the tropics and is mostly associated with ENSO.

While most of the radiative imbalance that changes enormously with seasons is offset by transports of energy between ocean and land, changes in storage of energy in the atmosphere contribute a modest amount and seasonal uptake of heat by land can exceed $20\,\mathrm{W\,m^{-2}}$ over extratropical continents as a whole. This heat goes into warming the land, melting snow, and evaporating moisture. While the continental values seem reasonable, maps of the local values do not, at this point, but it is worthwhile examining this aspect using climate models to improve the observational estimates, provide a basis for evaluating surface fluxes, and improve models.

There is an interesting upward trend in latent energy and thus moisture from ocean to land in all reanalyses (Fig. 3). In ERA-I it amounts to about 0.6 PW from 1980 to the 2000s (Fig. 5) and this is equivalent to $0.14\,\mathrm{mm\,day^{-1}}$ change over that period (about $50\,\mathrm{mm\,yr^{-1}}$). This means an implied increasing excess of P over E. While land precipitation does not appear to have changed much in GPCP from 1979 to 2008 (Huffman et al. 2009), it has increased in several other products as seen in the recent annual *State of the Climate* assessment analysis (Parker et al. 2012). The main increase is from 1992 to 1999 and with an overall increase from the 1980s to 2000s in GPCC of about $15\,\mathrm{mm\,yr^{-1}}$ relative to GPCP. Jung et al. (2010) found similar trends in ET on land of $7.1\,\mathrm{mm\,yr^{-1}\,decade^{-1}}$ from 1979 to 1997 but stabilizing thereafter. The moisture budgets of reanalyses are known to suffer from spurious changes over time associated with changes in the observing system and especially the TOVS/ATOVS transitions in 1998 and 2001 (see Trenberth et al. 2011). ERA-I was mainly affected by changes in Special Sensor Microwave Imager (SSM/I) observations, and a noticeable discontinuity occurs early in 1992 in association with a huge increase in SSM/I data with the introduction of the *F10* Defense Meteorological Satellite Program (DMSP) satellite (see Trenberth et al. 2011). In all cases, these changes affected values mainly over the oceans, but this affects the moisture flow onto land. Hence it seems likely that the large trend (Fig. 5) is at least partly spurious. It would be reduced by about half (0.3 PW or $25\,\mathrm{mm\,yr^{-1}}$) if the LE values prior to 1992 were increased by about 0.3 PW as part of a step function, and DSE would need to be decreased by a similar amount. However, a warmer ocean and higher precipitable water over the oceans (Trenberth et al. 2005) provides a viable mechanism for an increased transport of water onto land as part of an intensified water cycle. Increases in La Niña events have also contributed.

The net annual mean land energy imbalance ranges from 0.2 to $4.3\,\mathrm{W\,m^{-2}}$ in magnitude, which means all values are less than 2% of the mean of ASR and OLR as an indication of the net flow of energy through the climate system. For water, the net annual mean land residual ranges up to $-0.35\,\mathrm{mm\,day^{-1}}$ for Australia, where it is 20% of the precipitation value. All other values are less than 12%. Mean monthly residuals for water can be as large as about $0.3\,\mathrm{mm\,day^{-1}}$, and this may well be exacerbated by the lack of runoff data that is for the same time interval as indicated by the change in water storage owing to earlier snowmelt associated with climate change (Derksen and Brown 2012).

For the water budget, river discharge data updates are desired that extend beyond individual basins, GRACE

data need to be continually exercised and improved, and precipitation and ET estimates also require attention. Since this study was completed, a new release was made of GRACE data, version RL05, and products from three groups are available [from the Jet Propulsion Laboratory, as given by Landerer and Swenson (2012); University of Texas, as given by Tapley et al. (2004); and German Research Center for Geosciences (GFZ) Potsdam, as given by Siemes et al. (2013)]. We have recomputed all of our results with these new products, which all have differences between them in the mean monthly values for the regions in Figs. 8–12 on the order of 0.1–0.2 mm day^{-1}, and with the product used here, but none achieves closure in the surface water budget that is significantly improved upon our original estimate. Nonetheless, the different results highlight the uncertainties remaining in the GRACE products.

Pan et al. (2012) provide a comprehensive analysis of sources of error in their water budgets of river basins around the world. They suggest that ET is the biggest source of error in most basins, especially in southern Asia, Africa, and Australia, while precipitation is a major source of error in South America because of the heavy rainfall but sparse network of gages. These findings are consistent with our independent assessment. However, the use of the atmospheric moisture transports and their convergence provides a valuable large-scale constraint that makes many aspects of this problem now more viable.

Acknowledgments. This research is partially sponsored by NASA Grant NNX09AH89G.

REFERENCES

Albergel, C., P. De Rosnay, G. Balsamo, L. Isaksen, and J. Muñoz-Sabater, 2012: Soil moisture analyses at ECMWF: Evaluation using global ground-based in situ observations. *J. Hydrometeor.,* **13,** 1442–1460.

Balmaseda, M. A., K. E. Trenberth, and E. Källén, 2013: Distinctive climate signals in reanalysis of global ocean heat content. *Geophys. Res. Lett.,* **40,** 1754–1759, doi:10.1002/grl.50382.

Boening, C., J. K. Willis, F. W. Landerer, R. S. Nerem, and J. Fasullo, 2012: The 2011 La Niña: So strong, the oceans fell. *Geophys. Res. Lett.,* **39,** L19602, doi:10.1029/2012GL053055.

Bosilovich, M. G., F. R. Robertson, and J. Chen, 2011: Global energy and water budgets in MERRA. *J. Climate,* **24,** 5721–5739.

Dai, A., and K. E. Trenberth, 2002: Estimates of freshwater discharge from continents: Latitudinal and seasonal variations. *J. Hydrometeor.,* **3,** 660–687.

——, T. Qian, K. E. Trenberth, and J. D. Milliman, 2009: Changes in continental freshwater discharge from 1949 to 2004. *J. Climate,* **22,** 2773–2791.

Dee, D., and Coauthors, 2011: The ERA Interim reanalysis: Configuration and performance of the data assimilation system. *Quart. J. Roy. Meteor. Soc.,* **137,** 553–597, doi:10.1002/qj.828.

Derksen, C., and R. Brown, 2012: Spring snow cover extent reductions in the 2008–2012 period exceeding climate model projections. *Geophys. Res. Lett.,* **39,** L19504, doi:10.1029/2012GL053387.

Fasullo, J. T., and K. E. Trenberth, 2008a: The annual cycle of the energy budget. Part I: Global mean and land–ocean exchanges. *J. Climate,* **21,** 2297–2312.

——, and ——, 2008b: The annual cycle of the energy budget. Part II: Meridional structures and poleward transports. *J. Climate,* **21,** 2313–2325.

Gu, G., R. F. Adler, G. J. Huffman, and S. Curtis, 2007: Tropical rainfall variability on interannual-to-interdecadal and longer time scales derived from the GPCP monthly product. *J. Climate,* **20,** 4033–4046.

Hansen, J., M. Sato, P. Kharecha, and K. von Schuckmann, 2011: Earth's energy imbalance and implications. *Atmos. Chem. Phys.,* **11,** 13 421–13 449, doi:10.5194/acp-11-13421-2011.

Huffman, G. J., R. F. Adler, D. T. Bolvin, and G. Gu, 2009: Improving the global precipitation record: GPCP version 2.1. *Geophys. Res. Lett.,* **36,** L17808, doi:10.1029/2009GL040000.

Jiménez, C., and Coauthors, 2011: Global intercomparison of 12 land surface heat flux estimates. *J. Geophys. Res.,* **116,** D02102, doi:10.1029/2010JD014545.

Jung, M., and Coauthors, 2010: Recent decline in the global land evapotranspiration trend due to limited moisture supply. *Nature,* **467,** 951–954.

Landerer, F. W., and S. C. Swenson, 2012: Accuracy of scaled GRACE terrestrial water storage estimates. *Water Resour. Res.,* **48,** W04531, doi:10.1029/2011WR011453.

Loeb, N. G., B. A. Wielicki, D. R. Doelling, G. L. Smith, D. F. Keyes, S. Kato, N. Manalo-Smith, and T. Wong, 2009: Toward optimal closure of the earth's top-of-atmosphere radiation budget. *J. Climate,* **22,** 748–766.

——, J. M. Lyman, G. C. Johnson, R. P. Allan, D. R. Doelling, T. Wong, B. J. Soden, and G. L. Stephens, 2012: Observed changes in top-of-the-atmosphere radiation and upper-ocean heating consistent within uncertainty. *Nat. Geosci.,* **5,** 110–113, doi:10.1038/ngeo1375.

Lorenz, C., and H. Kunstmann, 2012: The hydrological cycle in three state-of-the-art reanalyses: Intercomparison and performance analysis. *J. Hydrometeor.,* **13,** 1397–1420.

Mueller, B., and Coauthors, 2011: Evaluation of global observations based evapotranspiration datasets and IPCC AR4 simulations. *Geophys. Res. Lett.,* **38,** L06402, doi:10.1029/2010GL046230.

Pan, M., A. K. Sahoo, T. J. Troy, R. K. Vinukollu, J. Sheffield, and W. F. Wood, 2012: Multisource estimation of long-term terrestrial water budget for major global river basins. *J. Climate,* **25,** 3191–3206.

Parker, D. E., K. Hilburn, P. Hennon, and A. Becker, 2012: Precipitation [In "State of the climate in 2011"]. *Bull. Amer. Meteor. Soc.,* **93,** S26–S27.

Rienecker, M. M., and Coauthors, 2011: MERRA: NASA's Modern-Era Retrospective Analysis for Research and Applications. *J. Climate,* **24,** 3624–3648.

Robertson, F. R., M. Bosilovich, J. Chen, and T. Miller, 2011: The effect of satellite observing system changes on MERRA water and energy fluxes. *J. Climate,* **24,** 5197–5217.

Sahoo, A. K., M. Pan, T. J. Troy, R. K. Vinukollu, J. Sheffield, and E. F. Wood, 2011: Reconciling the global terrestrial water budget using satellite remote sensing. *Remote Sens. Environ.,* **115,** 1850–1865.

Schneider, U., A. Becker, P. Finger, A. Meyer-Christoffer, M. Ziese, and B. Rudolf, 2013: GPCC's new land-surface precipitation climatology based on quality-controlled in-situ

data and its role in quantifying the global water cycle. *Theor. Appl. Climatol.,* doi:10.1007/s00704-013-0860-x, in press.

Siemes, C., P. Ditmar, R. E. M. Riva, D. C. Slobbe, X. L. Liu, and H. H. Farahani, 2013: Estimation of mass change trends in the Earth's system on the basis of GRACE satellite data, with application to Greenland. *J. Geod.,* **87,** 69–87, doi:10.1007/s00190-012-0580-5.

Solomon, S., D. Qin, M. Manning, Z. Chen, M. Marquis, K. Averyt, M. Tignor, and H. L. Miller Jr., Eds., 2007: *Climate Change 2007: The Physical Science Basis*. Cambridge University Press, 996 pp.

Syed, T. H., J. S. Famiglietti, and D. P. Chambers, 2009: GRACE-based estimates of terrestrial freshwater discharge from basin to continental scales. *J. Hydrometeor.,* **10,** 22–40.

——, ——, ——, J. K. Willis, and K. Hilburn, 2010: Satellite-based global-ocean mass balance estimates of interannual variability and emerging trends in continental freshwater discharge. *Proc. Natl. Acad. Sci. USA,* **42,** 17 916–17 921, doi:10.1073/pnas.1003292107.

Tapley, B. D., S. Bettadpur, M. Watkins, and C. Reigber, 2004: The gravity recovery and climate experiment: Mission overview and early results. *Geophys. Res. Lett.,* **31,** L09607, doi:10.1029/2004GL019920.

Trenberth, K. E., 2009: An imperative for climate change planning: tracking Earth's global energy. *Curr. Opin. Env. Sustainability,* **1,** 19–27, doi:10.1016/j.cosust.2009.06.001.

——, and D. P. Stepaniak, 2003a: Covariability of components of poleward atmospheric energy transports on seasonal and interannual timescales. *J. Climate,* **16,** 3691–3705.

——, and ——, 2003b: Seamless poleward atmospheric energy transports and implications for the Hadley circulation. *J. Climate,* **16,** 3706–3722.

——, and A. Dai, 2007: Effects of Mount Pinatubo volcanic eruption on the hydrological cycle as an analog of geoengineering. *Geophys. Res. Lett.,* **34,** L15702, doi:10.1029/2007GL030524.

——, and J. T. Fasullo, 2008: An observational estimate of ocean energy divergence. *J. Phys. Oceanogr.,* **38,** 984–999.

——, and ——, 2010: Tracking Earth's energy. *Science,* **328,** 316–317.

——, and ——, 2013: North American water and energy cycles. *Geophys. Res. Lett.,* **40,** 365–369, doi:10.1002/grl.50107.

——, ——, and L. Smith, 2005: Trends and variability in column-integrated water vapor. *Climate Dyn.,* **24,** 741–758.

——, and Coauthors, 2007a: Observations: Surface and atmospheric climate change. *Climate Change 2007: The Physical Science Basis,* S. Solomon et al., Eds., Cambridge University Press, 235–336.

——, L. Smith, T. Qian, A. Dai, and J. Fasullo, 2007b: Estimates of the global water budget and its annual cycle using observational and model data. *J. Hydrometeor.,* **8,** 758–769.

——, J. T. Fasullo, and J. Kiehl, 2009: Earth's global energy budget. *Bull. Amer. Meteor. Soc.,* **90,** 311–323.

——, ——, and J. Mackaro, 2011: Atmospheric moisture transports from ocean to land and global energy flows in reanalyses. *J. Climate,* **24,** 4907–4924.

van der Ent, R. J., H. H. G. Savenije, B. Schaefli, and S. C. Steele-Dunne, 2010: Origin and fate of atmospheric moisture over continents. *Water Resour. Res.,* **46,** W09525, doi:10.1029/2010WR009127.

Vinukollu, R. K., R. Meynadier, J. Sheffield, and E. F. Wood, 2011: Multi-model, multi-sensor estimates of global evapotranspiration: Climatology, uncertainties and trends. *Hydrol. Processes,* **25,** 3993–4010.